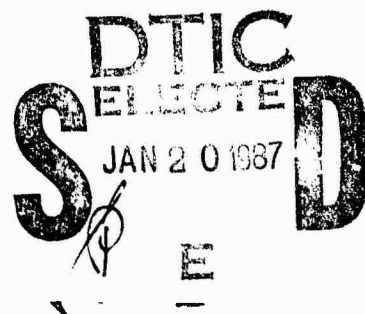# Communications Research Centre

AD-A176 069

THE IN-SITU CALIBRATION OF A

BILATERAL SPACE-FED PHASED

ARRAY ANTENNA

by

E.K.L. Hung, N.R. Fines, R.M. Turner

CRC REPORT NO. 1370
OTTAWA, JUNE 1983

Government of Canada
Department of Communications

Gouvernement du Canada
Ministère des Communications

Canadä

87   1

COMMUNICATIONS RESEARCH CENTRE

DEPARTMENT OF COMMUNICATIONS
CANADA

THE IN-SITU CALIBRATION OF A BILATERAL SPACE-FED PHASED ARRAY ANTENNA

by

E.K.L. Hung, N.R. Fines, R.M. Turner

(Radar and Communications Technology Branch)

DTIC
ELECTE
NOV 5 1986
S   D
B

CRC REPORT NO. 1370

June 1983
OTTAWA

TABLE OF CONTENTS

THE IN-SITU CALIBRATION OF A BILATERAL

SPACE-FED PHASED ARRAY ANTENNA

by

Eric K.L. Hung
N. Ross Fines
and
Ross M. Turner

June 1983

ABSTRACT

This report describes an in-situ technique to estimate the following parameters of a phased-array antenna:

1. the relative array-element excitation voltages,
2. the array-element tuning phases, and
3. the RF phase shifts at the array elements.

This technique has several significant features. First, it involves the use of two auxiliary antennas. One is a remote CW source directed at the phased-array antenna. The other is a passive antenna mounted close to the phased-array antenna. Its output is used to produce a reference phase for phase measurements. Second, it contains a technique to reduce the errors in phase estimates. Third, it takes note that beam steering uses phase sums of the form $(\phi_k + \beta_{k\ell})$, where ϕ_k is the tuning phase for the k-th array element and $\beta_{k\ell}$ is an RF phase shift of the array element, and pays special attention to reduce the errors associated with the estimates of these sums. Fourth, it assumes the use of a reasonably stable and strong CW source of commercially available quality. No other assumptions are made.

Experimental results obtained with a 295-element S-band space-fed phased-array antenna are given.

2

I. INTRODUCTION

A phased-array antenna requires periodic measurements of the following parameters:

1. the relative array-element excitation voltages,
2. the array-element tuning phases, and
3. the RF phase shifts at the array elements.

These parameters are needed to compensate for known and unknown variations in the array-element characteristics, the antenna geometry, and the antenna orientation. This task is preferably carried out in the background, so that it does not interfere with the normal operations of the antenna. The measurement technique is necessarily in-situ, and should be fast, interruptable, and not involve the use of an aperture probe if the antenna is to be returned to operation in small fractions of a second.

Several techniques which can be used to estimate the above array-element parameters under the conditions specified have been published in the open literature. Notable examples are those described in the papers by Lowenschuss [1], Hüschelrath and Sander [2], and Alexander and Gray [3]. Lowenschuss uses an auxiliary antenna in the far-field zone of the array antenna. A cable links this source with the array receiver to provide a reference phase for phase measurement. Three assumptions are made: (i) the nominal 180° RF phase shift of each array element is close to the actual value; (ii) the change in excitation voltage at an array element can be neglected when a phase bit is changed; and (iii) the tuned state of an array element can be identified as one of the phase states of the array element. The RF phase shift estimation technique in [1] has been modified for estimation with antennas which contain thousands of elements by Kahrilas and Jahn [4] and by Blake, Schwartzman, and Esposito [5]. The descriptions of these modified techniques are very sketchy. Hüschelrath and Sander [2] use essentially the same reference phase generation technique as in [1]. They assume very accurate knowledge of the distances between the auxiliary antenna and the individual array elements. The technique is not described in detail in the reference. Alexander and Gray [3] use an auxiliary antenna in the far-field zone of the array antenna. They do not use a cable linkage between the auxiliary antenna and the array radar. Instead, when an array element is tested, the reference phase is identified as the phase of the sum contribution of all the other array elements. The three assumptions in [1] are also made.

There are both favourable and unfavourable features in each of the above reference phase generation techniques. The techniques in [1] and [2] produce reference phases which are almost perfectly synchronized with that of the signal at the auxiliary antenna. This is favourable for RF phase shift measurements. However, the auxiliary antenna in these techniques cannot be located far away from the array antenna. This is unfavourable for tuning phase measurements, because accurate distance measurements are needed to correct for wavefront sphericity. The technique in [3] uses an auxiliary antenna which can be located at a large

distance away from the array antenna. This is favourable for tuning phase measurements. However, the reference phase in this technique is derived from the antenna output signal. This is unfavourable for RF phase shift measurement, because any error in reference phase is added to the RF phase shift estimate.

The three assumptions made in [1] and [3] are usually not satisfied. It is not uncommon to have a difference of more than a few degrees between the nominal 180° RF phase shift and the actual value. It is also not uncommon to have a change of more than 10% in the excitation voltage at an array element when its phase state is changed. A 10% change in excitation voltage alone can lead to many degrees of error in RF phase shift estimates. The third assumption on tuning phase is valid only if the number of phase bits in the phase shifters is large. In the special case of 3-bit phase shifters, for example, the tuned state of an array element can deviate from the phase state of the element by up to 22.5° $(=180°/2^3)$. The technique in [2] is difficult to evaluate and implement, because not enough details are published in the paper.

This report describes a new technique to measure the relative excitation voltages, tuning phases, and RF phase shifts of the elements of a phased-array antenna. It has several significant features. First, it incorporates a new reference phase generation technique which has all the favourable features in [1], [2], and [3] and none of their unfavourable features. Second, it takes note that the phase states of an array element are related to each other and uses this property to reduce the errors in the phase estimates. Third, it takes note that beamforming uses phase sums of the form $(\phi_k+\beta_{k\ell})$, where ϕ_k is the tuning phase for the k-th array element and $\beta_{k\ell}$ is an RF phase shift of the array element, and pays special attention to reduce the errors associated with the estimates of these sums. Fourth, it assumes the use of a reasonably stable and strong CW source of commercially availble quality. No other assumptions are made.

There are seven sections in this paper. Section II describes the array antenna used to develop the new technique and the relationship among the RF phase shifts of its phase control modules. Section III contains the derivation of the equations used to estimate the excitation voltages, tuning phases, and RF phase shifts. Section IV discusses the errors associated with the phase estimates. Section V describes the experimental setup to generate a reference signal from a remote CW source and the measurement of phased-array antenna output signals. Section VI contains two examples on the estimation of excitation voltages, tuning phases, and RF phase shifts. The first uses a distortion-free space-fed phased-array antenna. The second uses a distorted antenna. Section VII contains concluding remarks.

II THE PHASED ARRAY-ANTENNA

The phased-array antenna used in the experimental verification of the estimation technique is on loan to the Canadian Department of National Defence from the Royal Signal and Radar Establishment, Malvern,

United Kingdom, under the auspices of the The Technical Cooperation Program. It is a reciprocal S-band antenna, consisting of a rectangular feed horn mounted 1.11 m behind a vertical planar array as shown in Figs. 1 and 2. The planar array contains 295 elements configured into an eliptical aperture with a 1.67 m horizontal axis and a 1.05 m vertical axis. In each array element is a 3-bit PIN-diode phase-control module attached to flared waveguide horns at the ends. The PIN diodes are used to switch three transmission line segments with nominal lengths 0.125, 0.25, and 0.5 wavelengths in and out of the signal path, thereby producing $2^3 = 8$ RF phase shifts. The RF phase shifts at the k-th array element are identified as $\{\beta_{k\ell}; \ell=0,1,2,\ldots,7\}$. They satisfy the relations

$$\beta_{k\ell} = 0 \quad , \qquad \ell=0 \quad , \tag{1}$$

$$\beta_{k\ell} \simeq \ell \times 45° \quad , \qquad \ell=1,2,4 \quad , \tag{2}$$

$$\beta_{k\ell} = \beta_{k1} + \beta_{k2} \quad , \qquad \ell=3 \quad , \tag{3}$$

and

$$\beta_{k\ell} = \beta_{k4} + \beta_{k(\ell-4)}, \quad \ell=5,6,7 \quad . \tag{4}$$

The independent RF phase shifts are β_{k1}, β_{k2}, and β_{k4}. Their actual values depend on the actual lengths of the nominal 0.125, 0.25, and 0.5 wavelength transmission lines, respectively, in the phase control module of the k-th array element.

III EQUATIONS

In this section, an expression for the antenna output due to a remote CW test source is given. The conditions for the measurement of antenna outputs are stated. Equations for the estimation of array-element excitation voltages, tuning phases, and RF phase shifts are then derived. A summary is given at the end.

A. Expression for Antenna Output Amplitude

The complex amplitude at the phased-array antenna output due to a remote CW source can be written as a sum of the contribution from a single specified array element plus a second term comprising all the other contributions,

$$A_{k\ell} = a_{k\ell}\, e^{j(\alpha_k+\beta_{k\ell})} + B_k \quad . \tag{5}$$

Here, k signifies the quantities associated with the specified element and ℓ signifies the phase state of this element. The elemental amplitude from this element has an effective magnitude $a_{k\ell}$. Its phase is α_k before phase shifting. Amplitude B_k represents the sum of all other contributions to $A_{k\ell}$. It includes the sum of elemental amplitudes from all other array elements, mutual coupling, and background noises.
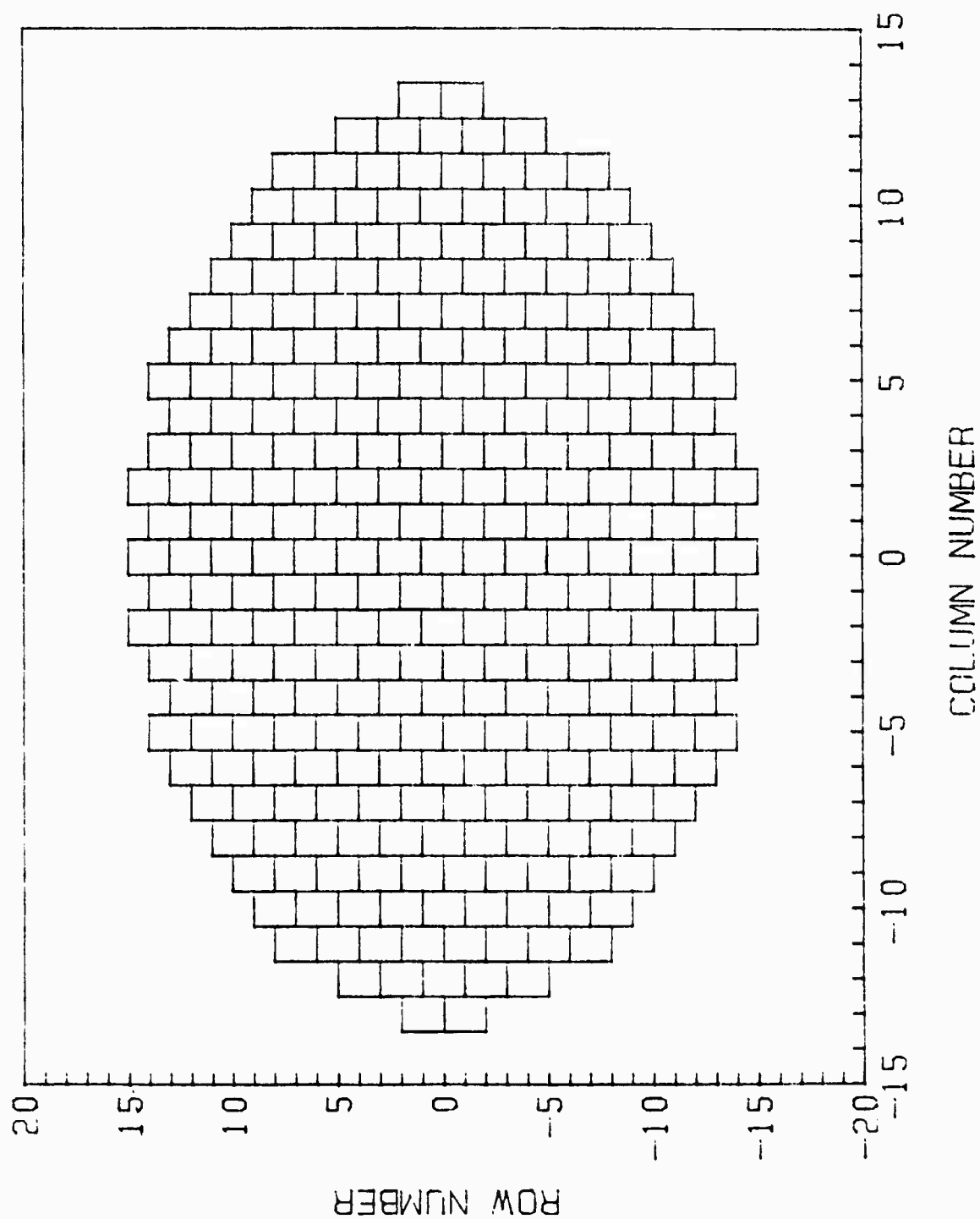
Fig. 1 Layout of array elements as seen from the back. The array has 295 elements configured into an elliptical aperture with a 1.67 m horizontal axis and a 1.05 m vertical axis.
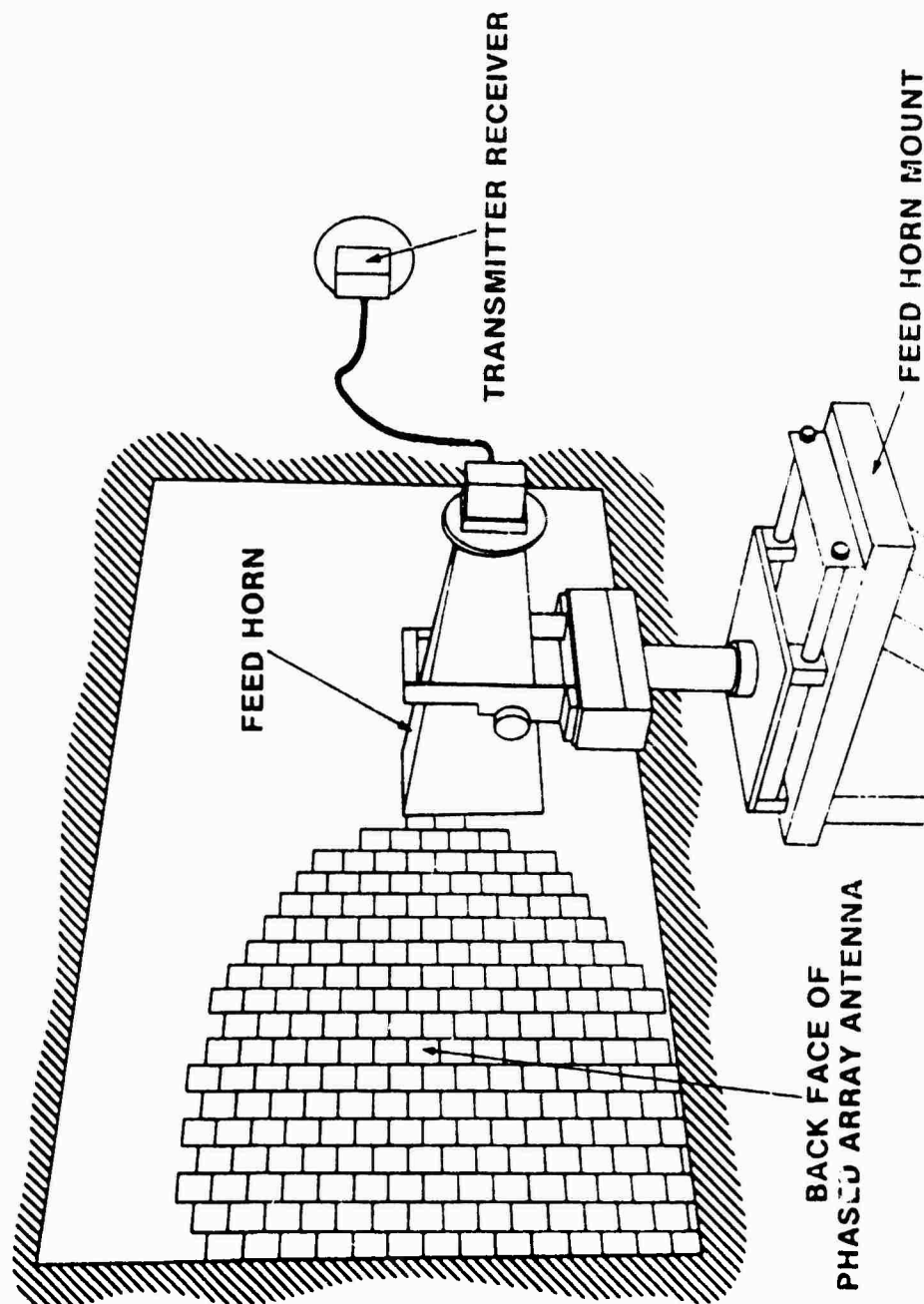
Fig. 2 Rear view of the space-fed phased-array antenna with the feed horn in position.

shown in Figure 3. Also shown in this figure are the tips of other amplitudes in the set $\{A_{k\ell}; \ell=1,2,\ldots,7\}$ in the special case of $a_{k\ell} = a_k$ and $\beta_{k\ell} = \ell \times 45°$. These tips lie on a circle of radius a_k. The complex amplitudes representing the contributions from the k-th array element are denoted by vectors radiating from the tip of B_k and terminating at the circumference of the circle.

Because the sum of α_k and $\beta_{k\ell}$ appears in the expression for $A_{k\ell}$ it is convenient to denote this sum as

$$\gamma_{k\ell} = \alpha_k + \beta_{k\ell} \quad . \tag{6}$$

From the properties of the $\beta_{k\ell}$ in (1) to (4), one has

$$\gamma_{k0} = \alpha_k \quad , \tag{7}$$

$$\gamma_{k\ell} - \gamma_{k0} = \beta_{k\ell}, \qquad \ell=0,1,2,\ldots,7 \quad , \tag{8}$$

$$\gamma_{k\ell} - \gamma_{k(\ell-4)} = \beta_{k4}, \quad \ell=4,5,6,7 \quad , \tag{9}$$

and

$$\gamma_{k1} + \gamma_{k2} = \gamma_{k0} + \gamma_{k3} \quad . \tag{10}$$

B. Assumptions

In the rest of this paper, it shall be assumed that $a_{k\ell}$, α_k and B_k are constants. This means that the experimental setup must be such that the following conditions are satisfied during amplitude measurement:

1. The output power of the CW source is sufficiently stable over the duration of an antenna calibration run.
2. The phase coherency between the CW source and the reference signal at the radar receiver is very high.
3. The magnitude of fluctuations in the noise background is small compared with $a_{k\ell}$.

The first condition is not difficult to satisfy. In practice a CW source with an output power which varies by less than 2% over the duration of a calibration run is good enough for amplitude measurements. This type of CW source is readily available commercially. The detailed experimental setup and the suppression of noises to satisfy the remaining two conditions are described in Section V.

Amplitude B_k includes the contribution due to mutual coupling among the array elements. Strictly speaking, it is also dependent on the phase-shift state ℓ of the k-th array element. However, this dependence on ℓ is very weak and can be ignored completely.
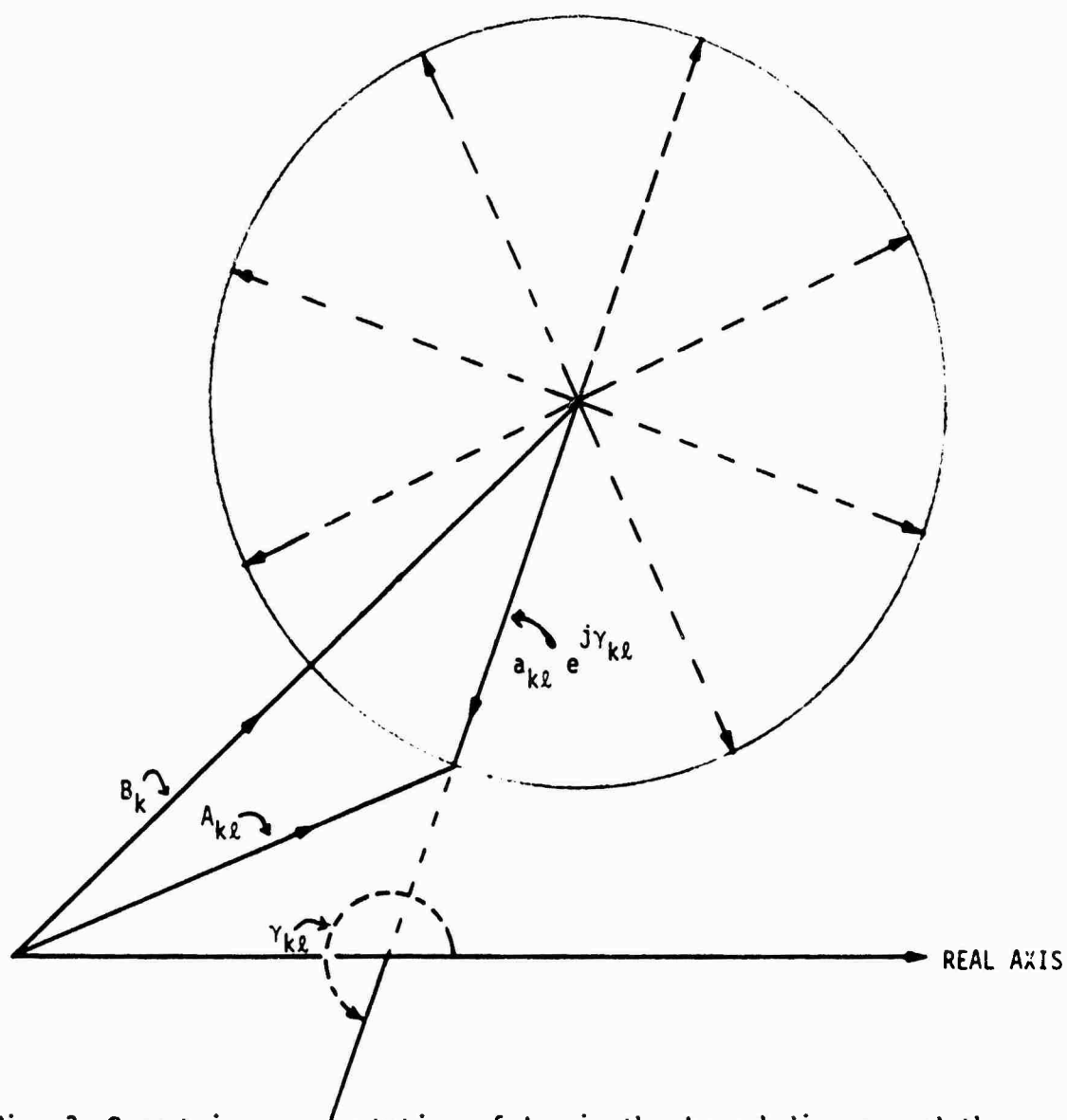
Fig. 3 Geometric representation of $A_{k\ell}$ in the Argand diagram and the tips of other complex amplitudes in the set $\{A_{k\ell};\ \ell=0,1,2,\ldots,7\}$ in the special case of $a_{k\ell}$ = constant and $\beta_{k\ell} = \ell \times 45°$. The tips of the complex amplitudes in the set lie on a circle centred at the tip of B_k. The vector drawn from the tip of B_k to the tip of $A_{k\ell}$ is the elemental amplitude from the k-th array element. The angle between this vector and the real axis is $\gamma_{k\ell}$, $\gamma_{k\ell} = \alpha_k + \beta_{k\ell}$.

C. Estimation of Relative Excitation Voltages

The value of $a_{k\ell}$ in (5) is dependent on both k and ℓ. It is dependent on k because the coupling between the feed horn and an array element is dependent on the position of the array element. It is dependent on ℓ, because the insertion loss at the k-th array element is dependent on the signal path specified by ℓ. Only the average value of the $a_{k\ell}$s over all the phase states of the k-th array element is of interest here. This average is dependent on how it is calculated. One method, suggested by Fig. 3, is to calculate it as

$\hat{a}_k$ = radius of the best-fit circle through the set of amplitudes $\{A_{k\ell};\ \ell=0,1,2,\dots,7\}$ in the Argand diagram. (11)

This radius is also the radius of the best-fit circle through the set of elemental amplitudes $\{a_{k\ell}e^{j\beta_{k\ell}};\ \ell=0,1,2,\dots,7\}$.

The estimate of relative excitation voltage at the k-th array element is defined here as

$$\hat{b}_k = \frac{\hat{a}_k}{\bar{a}}\ , \qquad k=1,2,3,\dots,295\ , \qquad (12)$$

where

$$\bar{a} = \frac{1}{K'}\sum{}'\hat{a}_k \qquad (13)$$

is a normalization constant, K' is the number of functioning elements, and $\sum'$ is a summation over the functioning elements. Thus the b_ks defined here satisfy the condition

$$\sum{}'\hat{b}_k = K' \quad ,$$

so that the average of the relative excitation voltages over all the functioning elements is unity. An array element is arbitrarily identified as a functioning element if a_k is larger than 30% of its theoretical value. This choice of threshold is based on the Section VI results to be presented later.

The position and the radius of the best-fit circle through $\{A_{k\ell};\ \ell=0,1,2,\dots,7\}$ are dependent on the criterion for the construction of this circle. It is convenient to define this circle as the circle which minimizes the cost function

$$S = \sum_{\ell=0}^{7} (d_{k\ell}^2 - a_k^2)^2 \quad , \qquad (15)$$

where $d_{k\ell}$ is the distance of $A_{k\ell}$ from the circle centre $\hat{B}_k$, an estimate of B_k. This cost function is chosen for ease of analysis and the fact that it leads to tractable closed form solutions. In Appendix A, it is shown that the coordinates of B_k can be calculated in closed form as

$$\text{Re}\{\hat{B}_k\} = [f(x,y)-g(x,y)]/h(x,y) \quad , \tag{16}$$

$$\text{Im}\{\hat{B}_k\} = [f(y,x)-g(y,x)]/h(x,y) \quad , \tag{17}$$

where

$$f(x,y) = 2(\overline{y^2}-\overline{y}\overline{y})(\overline{x^3}-\overline{x}\overline{x^2}+\overline{x}\overline{y^2}-\overline{x}\overline{y^2}) \quad , \tag{18}$$

$$g(x,y) = 2(\overline{xy}-\overline{x}\overline{y})(\overline{x^2y}-\overline{x^2}\overline{y}+\overline{y^3}-\overline{y}\overline{y^2}) \quad , \tag{19}$$

$$h(x,y) = 4[\overline{x^2}-\overline{x}\overline{x})(\overline{y^2}-\overline{y}\overline{y})-(\overline{xy}-\overline{x}\overline{y})^2] \quad , \tag{20}$$

and

$$\overline{x^u y^v} = \frac{1}{8} \sum_{\ell=0}^{7} [\text{Re}(A_{k\ell})]^u [\text{Im}(A_{k\ell})]^v \quad . \tag{21}$$

The radius of the circle is given by

$$\hat{a}_k = [\overline{x^2}+\overline{y^2}-2\overline{x}\text{Re}(\hat{B}_k)-2\overline{y}\text{Im}(\hat{B}_k)+|\hat{B}_k|^2]^{\frac{1}{2}} \quad . \tag{22}$$

D. Estimation of RF Phase Shifts

The RF phase shifts at the k-th array element are β_{k0}, β_{k1}, $\beta_{k2},\ldots,\beta_{k7}$. In the following, these phase shifts are estimated through the estimation of the $\gamma_{k\ell}$s given by (6). There are five steps in the procedure. First a set of initial estimates denoted by $\{\hat{\gamma}_{k\ell}^{(1)}; \ell=0,1,2,\ldots,7\}$ is constructed. Second, the estimate of B_{k4} is calculated. Third, condition (9) is imposed to produce a set of improved estimates $\{\hat{\gamma}_{k\ell}^{(2)}; \ell=0,1,2,\ldots,7\}$. Fourth, condition (10) is imposed to produce the final estimates $\{\hat{\gamma}_{k\ell}; \ell=0,1,2,\ldots,7\}$. Finally, estimates of β_{k1} and β_{k2} are calculated. Imposition of conditions (9) and (10) on the estimates of the $\gamma_{k\ell}$s leads to reductions in the errors in phase estimates. A discussion on this error reduction is given in Section IV.

To derive an initial estimate of the $\gamma_{k\ell}$s, it is noted that the phase of $(A_{k\ell} - B_k)$ can be identified as the initial estimate of $\gamma_{k\ell}$, i.e.,

$$\hat{\gamma}_{k\ell}^{(1)} = \text{phase } (A_{k\ell} - \hat{n}_k), \quad \ell = 0, 1, 2, \ldots, 7 \quad . \tag{23}$$

There are four values of phase difference given by $[\hat{\gamma}_{k(\ell+4)}^{(1)} - \hat{\gamma}_{k\ell}^{(1)}]$, $\ell = 0, 1, 2, 3$. According to (9), each can be used to obtain an estimate of β_{k4}. Because the nominal value of β_{k4} is $180°$, these four initial estimates of β_{k4}, identified with $\ell = 0$ to 3, can be calculated as

$$\hat{\beta}_{k4}^{(1)}(\ell) = \hat{\gamma}_{k(\ell+4)}^{(1)} - \hat{\gamma}_{k\ell}^{(1)} + n_{k\ell} \times 360° \quad , \tag{24}$$

where $n_{k\ell}$ is an integer which restricts $\hat{\beta}_{k4}^{(1)}(\ell)$ to the range $[0°, 360°)$ centred at the nominal value of β_{k4}. The final estimate of β_{k4} is defined as the average of the initial estimates,

$$\hat{\beta}_{k4} = \frac{1}{4} \sum_{\ell=0}^{3} \hat{\beta}_{k4}^{(1)}(\ell) \quad . \tag{25}$$

Condition (9) is then imposed through the construction of a new set of estimates, denoted by $\{\hat{\gamma}_{k\ell}^{(2)}; \ell = 0, 1, 2, \ldots, 7\}$ defined as

$$\hat{\gamma}_{k\ell}^{(2)} = \begin{cases} \hat{\gamma}_{k\ell}^{(1)} + 0.5[\hat{\beta}_{k4}^{(1)}(\ell) - \hat{\beta}_{k4}^{(1)}], & \ell = 0, 1, 2, 3 \quad , \\[1em] \hat{\gamma}_{k\ell}^{(1)} - 0.5[\hat{\beta}_{k4}^{(1)}(\ell-4) - \hat{\beta}_{k4}^{(1)}], & \ell = 4, 5, 6, 7 \quad . \end{cases} \tag{26}$$

It is a simple matter to verify that these improved estimates satisfy the relation

$$\hat{\gamma}_{k\ell}^{(2)} - \hat{\gamma}_{k(\ell-4)}^{(2)} = \hat{\beta}_{k4}, \quad \ell = 4, 5, 6, 7 \quad . \tag{27}$$

Relation (10) is imposed through the use of a two-step calculation procedure derived in Appendix B. Initially, a dummy phase angle is calculated as

$$\delta_k = \hat{\gamma}_{k1}^{(2)} + \hat{\gamma}_{k2}^{(2)} - \hat{\gamma}_{k0}^{(2)} - \hat{\gamma}_{k3}^{(2)} + p_k \times 360° \quad , \tag{28}$$

where p_k is an integer which restricts δ_k to the range $[-180°, 180°)$. This range is chosen because δ_k is zero if (10) is satisfied. The second step calculates the final estimates $\{\gamma_{k\ell}; \ell = 0, 1, 2, \ldots, 7\}$ as

$$\hat{\gamma}_{k\ell} = \hat{\gamma}_{k\ell}^{(2)} + \varepsilon_\ell \delta_k, \qquad \ell=0,1,2,\ldots,7 \quad . \qquad (29)$$

The e_ℓs are derived in Appendix B and are given by

$$e_\ell = \begin{cases} 0.25, & \ell=0,3,4,7, \\ -0.25, & \ell=1,2,5,6. \end{cases} \qquad (30)$$

Estimates of RF phase shifts, including $\hat{\beta}_{k0}$ and $\hat{\beta}_{k4}$, are calculated from the final estimates of the $\gamma_{k\ell}$s as

$$\hat{\beta}_{k\ell} = \hat{\gamma}_{k\ell} - \hat{\gamma}_{k0} + q_{k\ell} \times 360°, \qquad \ell=0,1,2,\ldots,7 \quad . \qquad (31)$$

Here $q_{k\ell}$ is an integer which restricts $\hat{\beta}_{k\ell}$ to the range $[(\ell \times 45° - 180°),$ $(\ell \times 45° + 180°))$. This range is centred at the nominal value, $\ell \times 45°$, of $\beta_{k\ell}$.

The $\hat{\beta}_{k4}$ calculated with (31) is the same as the $\hat{\beta}_{k4}$ calculated with (25). The $\beta_{k\ell}$s satisfy relations (1), (3) and (4), i.e.,

$$\hat{\beta}_{k\ell} = 0 , \qquad \ell=0 , \qquad (32)$$

$$\hat{\beta}_{k\ell} = \hat{\beta}_{k1} + \hat{\beta}_{k2}, \qquad \ell=3 , \qquad (33)$$

$$\hat{\beta}_{k\ell} = \hat{\beta}_{k4} + \hat{\beta}_{k(\ell-4)}, \qquad \ell=5,6,7 \quad . \qquad (34)$$

E. Estimation of Tuning Phase

The main beam of the array antenna is pointed at the remote CW source if all the elemental amplitudes from the array elements arrive at the feed horn with the same phase. In this case, the radar receiver output signal has the largest possible amplitude. Angle α_k in (5) is the phase of the k-th elemental signal at the radar receiver output. A phase reduction equal to α_k, equivalent to a phase advance of $(360° - \alpha_k)$, applied to the k-th elemental signal would force it to have a zero phase at the radar receiver output. If all the elemental amplitudes were to have zero phase at the radar receiver output, the radar receiver output would have the largest possible amplitude. Hence, apart from a constant common to all array elements, α_k is the phase reduction which must be applied to the k-th elemental amplitude to steer the main beam of the antenna at the remote CW source.

The theoretical value of α_k, denoted by α_k^T, can be calculated from the antenna geometry, the CW source direction relative to the antenna boresight direction, and the array-element insertion phases. The difference

$$\phi_k = \alpha_k - \alpha_k^T \tag{35}$$

is the tuning phase for the k-th array element. From (7), an estimate of α_k is given by

$$\hat{\alpha}_k = \hat{\gamma}_{k0} \quad . \tag{36}$$

Therefore an estimate of ϕ_k is

$$\hat{\phi}_k = \hat{\gamma}_{k0} - \alpha_k^T \quad . \tag{37}$$

F. Summary

Let $\{A_{k\ell}; k=1,2,3,\ldots,295; \ell=0,1,2,\ldots,7\}$ be the phased array antenna outputs measured with a remote CW source. The estimation of relative array-element excitation voltages, tuning phases, and RF phase shifts can be carried out in eight steps:

Step 1 Set k=0

Step 2 Replace k by k+1

Step 3 Calculate circle radius a_k and circle centre $\hat{B}_k$ with (16) to (22)

Step 4 Calculate $\{\hat{\gamma}_{k\ell}^{(1)}; \ell=0,1,2,\ldots,7\}$ with (23)

Calculate $\{\hat{\gamma}_{k\ell}^2 ; \ell=0,1,2,\ldots,7\}$ with (24) to (26)

Calculate $\{\hat{\gamma}_{k\ell}; \ell=0,1,2,\ldots,7\}$ with (28) to (30)

Calculate estimates of RF phase shifts $\{\hat{\beta}_{k\ell}; \ell=0,1,2,\ldots,7\}$ with (31)

Step 5 Calculate the estimate of tuning phase ϕ_k with (37)

Step 6 If k=295 proceed directly to Step 8

Step 7 Return to Step 2

Step 8 Calculate the estimates of the relative array-element excitation voltages $\{b_k; k=1,2,3,\ldots,295\}$ with (12) and (13).

The estimates $\hat{a}_k$, $\hat{\alpha}_k$, and the $\hat{\beta}_{k\ell}$s can be checked in two places. First the $\beta_{k4}^{(1)}(\ell)$s calculated in (24) must be close to 180°. Second, the

14

δ_k calculated with (28) must be close to zero, because its expected value is zero.

IV ERRORS IN PHASE ESTIMATES

Let the initial estimates given by (23) be related to the correct values by

$$\hat{\gamma}_{k\ell}^{(1)} = \gamma_{k\ell} + \epsilon_{k\ell} \quad , \tag{38}$$
$$k = 1,2,3,\ldots,295 \quad ,$$
$$\ell = 0,1,2,\ldots,7 \quad ,$$

where $\epsilon_{k\ell}$ is the error in the initial estimate of $\gamma_{k\ell}$. The statistical properties of the $\epsilon_{k\ell}$s have been studied with computer simulations. The results show that, for a given array element, the errors are independent, have zero mean, and the same variance, i.e.

$$E\{\epsilon_{k\ell}\} = 0 \quad , \tag{39}$$

$$E\{\epsilon_{k\ell}\epsilon_{k\ell'}\} = \begin{cases} 0, & \ell \neq \ell , \\ \sigma_k^2 , & \ell = \ell' , \end{cases} \tag{40}$$

$$\ell,\ell'=0,1,2,\ldots,7 \quad .$$

The variance of $\epsilon_{k\ell}$ depends on k. Usually, it is smaller if the element excitation voltage is larger.

From (24) to (30), one can show that the estimates of the independent RF phase shifts are related to the correct values by

$$\hat{\beta}_{k1} = \beta_{k1} + 0.25(-\epsilon_{k0}+\epsilon_{k1}-\epsilon_{k2}+\epsilon_{k3}-\epsilon_{k4}+\epsilon_{k5}-\epsilon_{k6}+\epsilon_{k7}) \quad , \tag{41}$$

$$\hat{\beta}_{k2} = \beta_{k2} + 0.25(-\epsilon_{k0}-\epsilon_{k1}+\epsilon_{k2}+\epsilon_{k3}-\epsilon_{k4}-\epsilon_{k5}+\epsilon_{k6}+\epsilon_{k7}) \quad , \tag{42}$$

$$\hat{\beta}_{k4} = \beta_{k4} + 0.25(-\epsilon_{k0}-\epsilon_{k1}-\epsilon_{k2}-\epsilon_{k3}+\epsilon_{k4}+\epsilon_{k5}+\epsilon_{k6}+\epsilon_{k7}) \quad . \tag{43}$$

These expressions, together with (39) and (40), show that $\hat{\beta}_{k1}$, $\hat{\beta}_{k2}$ and B_{k4} are unbiased estimates,

$$E\{\hat{\beta}_{k\ell}\} = \beta_{k\ell} , \tag{44}$$

with variances

$$\text{var}\{\hat{\beta}_{k\ell}\} = 0.5\sigma_k^2 \qquad \ell=1,2,4 \quad . \tag{45}$$

The estimate of the tuning phase is related to the correct value ϕ_k by

$$\hat{\phi}_k = \phi_k + (\hat{\gamma}_{k0} - \gamma_{k0})$$

$$= \phi_k + 0.25(2\varepsilon_{k0} + \varepsilon_{k1} + \varepsilon_{k2} + \varepsilon_{k4} - \varepsilon_{k7}) \quad . \tag{46}$$

The first line on the right hand side of this expression is derived with (7), (35), and (37). The second line is derived with (38) and (24)-(30). This estimate is unbiased,

$$E\{\hat{\phi}_k\} = \phi_k \quad , \tag{47}$$

and has variance

$$\text{var}\{\hat{\phi}_k\} = 0.5\sigma_k^2 \quad . \tag{48}$$

Phase sums $\{(\phi_k + \beta_{k\ell}); \ k=1,2,3,\ldots,295; \ \ell=0,1,2,\ldots,7\}$ are used in beam steering. For example, to steer a beam at the remote CW source, the phase state, identified as $\ell(k)$, at the k-th array element must be such that $(\phi_k + \beta_{k\ell(k)})$ is closer to $-\alpha_k^T$ than any other phase sum in the set $\{(\phi_k + \beta_{k\ell}); \ \ell=0,1,2,\ldots,7\}$. The estimates of the phase sums can be calculated as

$$(\phi_k \hat{+} \beta_{k\ell}) = \hat{\phi}_k + \hat{\beta}_{k\ell} \quad , \tag{49}$$

$$k=1,2,3,\ldots,295 \quad ,$$
$$\ell=0,1,2,\ldots,7 \quad .$$

Using relations (1)-(4), (32)-(34), and (41)-(46), one can show that these estimates are unbiased,

$$E\{(\phi_k \hat{+} \beta_{k\ell})\} = \phi_k + \beta_{k\ell} \quad , \tag{50}$$

and have variances

$$\text{var}\{(\phi_k \hat{+} \beta_{k\ell})\} = 0.5\sigma_k^2 \quad . \tag{51}$$

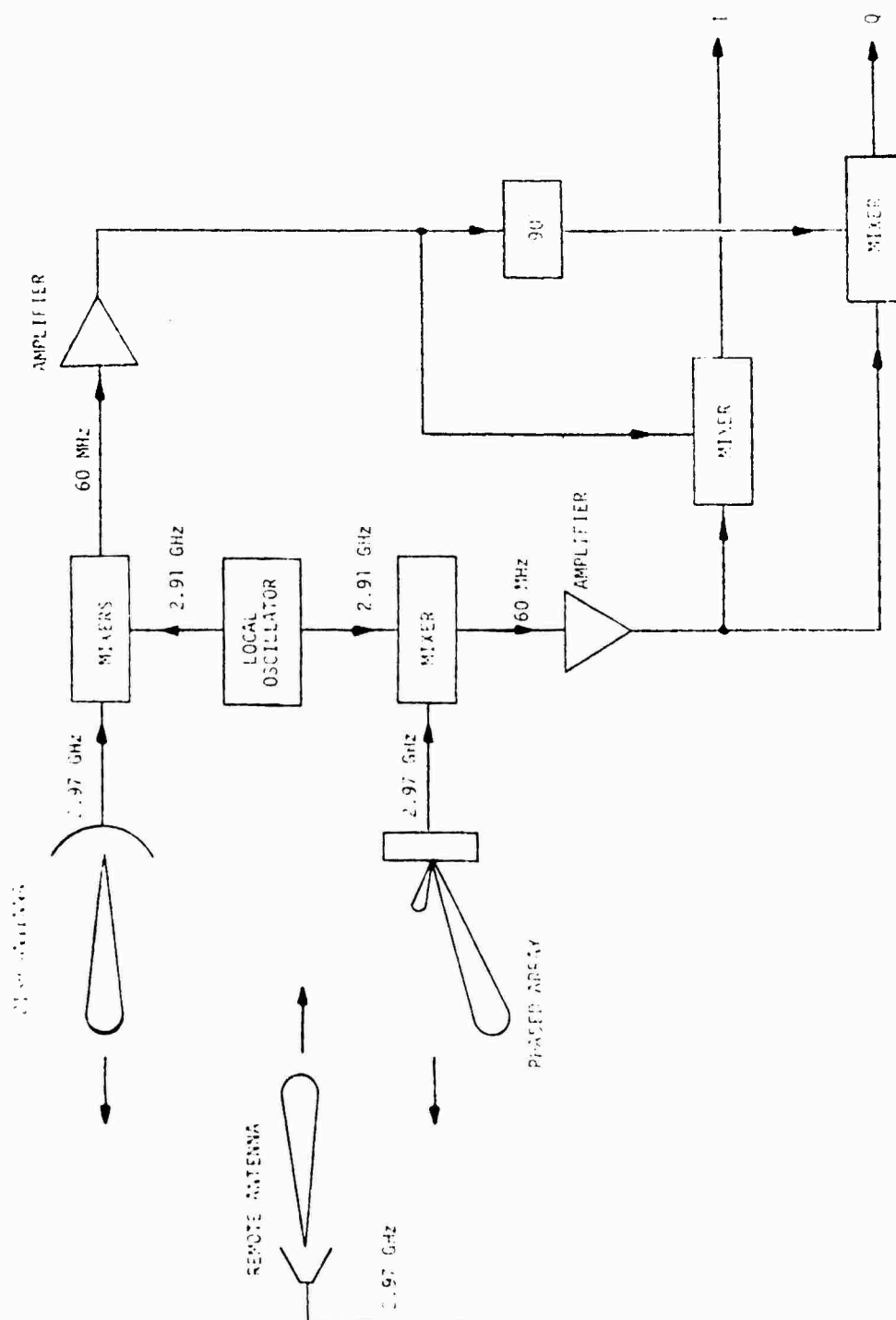For example, the estimate of $(\phi_k + \beta_{k7})$ can be calculated with (44),

Fig. 4 Experimental setup to measure the output of the phased-array
antenna. The CW source was slightly over one kilometre in front
of the phased-array antenna. The dish antenna was located at a
distance of about 7 metres from the phased-array antenna. Its
output was used as a reference signal for the quadrature sampling
of the phased-array antenna output.

Step 1

Set up the experiment as shown in Fig. 5. Steer the CW source at the phased-array antenna. Steer the dish antenna at the source. Steer the phased-array beam away from the source to make the initial I and Q channel outputs as small as possible.

Step 2

Set k=0.

Step 3

Replace k by k+1.

Step 4

Cycle the k-th array element through all its eight phase states. Take M individual antenna output amplitudes at each phase state. Identify the m-th amplitude at the ℓ-th phase state as $D_{k\ell}(m)$.

Step 5

Return the k-th array element to its original phase state, i.e., the phase state at the end of Step 1.

Step 6

If k=295, proceed directly to Step 8.

Step 7

Return to Step 3.

Step 8

Calculate $A_{k\ell}$ as

$$A_{k\ell} = \frac{1}{M} \sum_{m=1}^{M} D_{k\ell}(m) \quad , \tag{56}$$

$$k=1,2,3,\ldots,295 \quad ,$$
$$\ell=0,1,2,\ldots,7 \quad .$$

A choice M=2000 was made. This choice produced estimates $\hat{\beta}_{k1}$, $\hat{\beta}_{k2}$, $\hat{\beta}_{k4}$, and ϕ_k which had standard deviations less than 0.25 degree in repeated measurements with the central element in the array. This central element was identified with k=148 (see also Table I).

VI   RESULTS

The results of two experiments to estimate relative excitation voltages, tuning phases, and RF phase shifts are presented here. The first was carried out with a distortion-free phased-array antenna. The second was carried out with the feed horn rotated to provide an example of calibration with a distorted antenna.

A. Distortion-Free Antenna

Fig. 5 shows the best-fit circle through the set of complex amplitudes $\{A_{k\ell}; k=148; \ell=0,1,2,\ldots,7\}$ measured with the central element, identified with $k = 148$, cycled through all its RF phase states. The tips of the $A_{k\ell}$s are marked with crosses labelled with ℓ. The positions of the crosses relative to the circle might suggest that the gain for the I-channel output (real component of the $A_{k\ell}$s) should be increased. This modification of the I-channel gain was not carried out, because the complex amplitudes measured with other array elements did not support this gain modification.

The estimated values of the relative excitation voltages are plotted in Fig. 6. They were in good agreement with the theoretical values. The voltages in the centre of the array were relatively larger than those near the edges, because the feed horn was closest to, and pointed at, the centre element. The dots in the figure denote the positions of the defective elements. The excitation voltages at these elements were less than 10% of the theoretical values. The excitation voltages at the other elements were more than 50% of the theoretical values.

Listed in Table I are some RF phase shifts obtained both by estimation and by bench measurements. Array elements k=128, 148, and 175 were in the centre of the middle column, identified as column 0. Elements k=141 and 168 were the two elements in the extreme right column, identified as column 13, when the array was viewed from the back. The estimated RF phase shifts deviated from the bench-measured values by $5°$ or less. The average deviation was slightly less than $2.5°$. This agreement was very much better than expected, because the bench measurements were carried out with a differenct CW source about twenty months earlier. Since then, the array had been disassembled and reassembled at least twice.

The estimates of array-element tuning phases were examined indirectly by sweeping a beam across the CW source. The results are shown in Fig. 7. Here, the solid curve was the antenna pattern constructed with estimated values of $\beta_{k\ell}$ and $\phi_{k\ell}$. The broken curve was constructed with ideal values defined as $\beta_{k\ell} = \ell \times 45°$ and $\phi_k = 0°$. There is no significant difference between the antenna patterns.

B. Distorted Antenna

The distorted antenna is shown in Fig. 8. The feed horn was pointed at the left edge of the array. The new results on relative excitation voltages and antenna patterns are shown in Figs. 9 and 10, respectively. In Fig. 9, the excitation voltages on the left of the array are larger than those on the right. In Fig. 10, the peak of the antenna pattern constructed with ideal values $\beta_{k\ell}$ and ϕ_k is on the left of the correct position. The widths of the peaks in the two antenna patterns are also larger than those in Fig. 7.
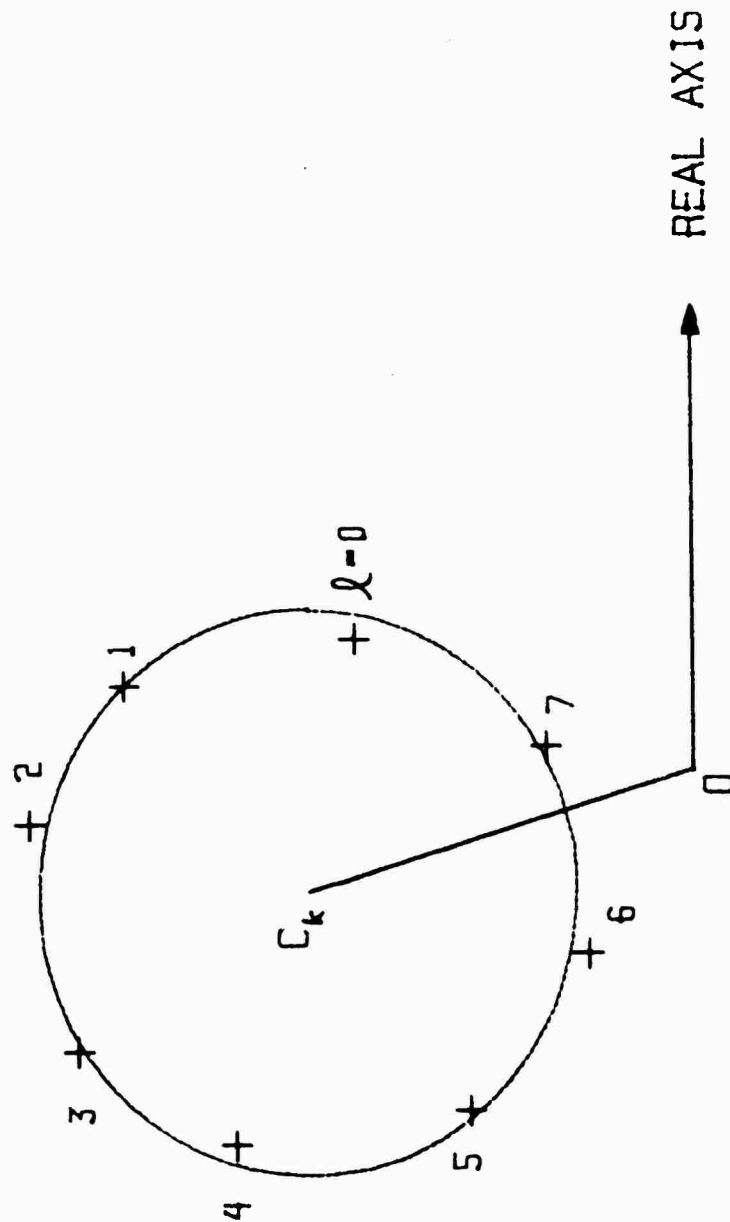
Fig. 5 The best-fit circle through the set of complex amplitudes
$\{A_{k\ell};\ k=148;\ \ell=0,1,2,\ldots,7\}$ measured with the central element
cycled through all its phase states. The tips of the $A_{k\ell}$s are
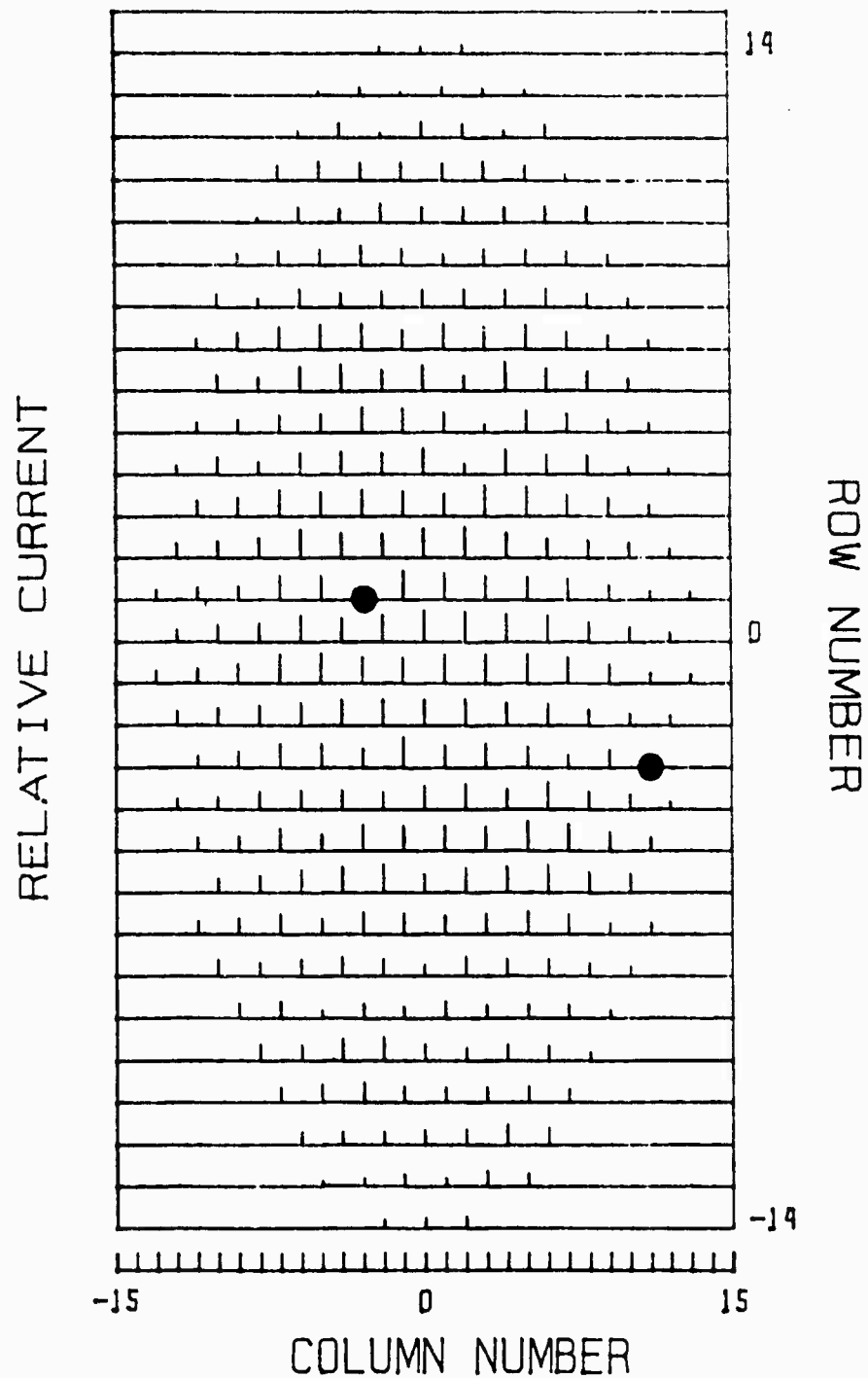marked by crosses labelled with ℓ.

Fig. 6 Estimates of relative array-element excitation voltages. The dots
denote the positions of the defective elements. The excitation
voltages at these defective elements were less than 10% of the
theoretical values. The excitation voltages at the functioning
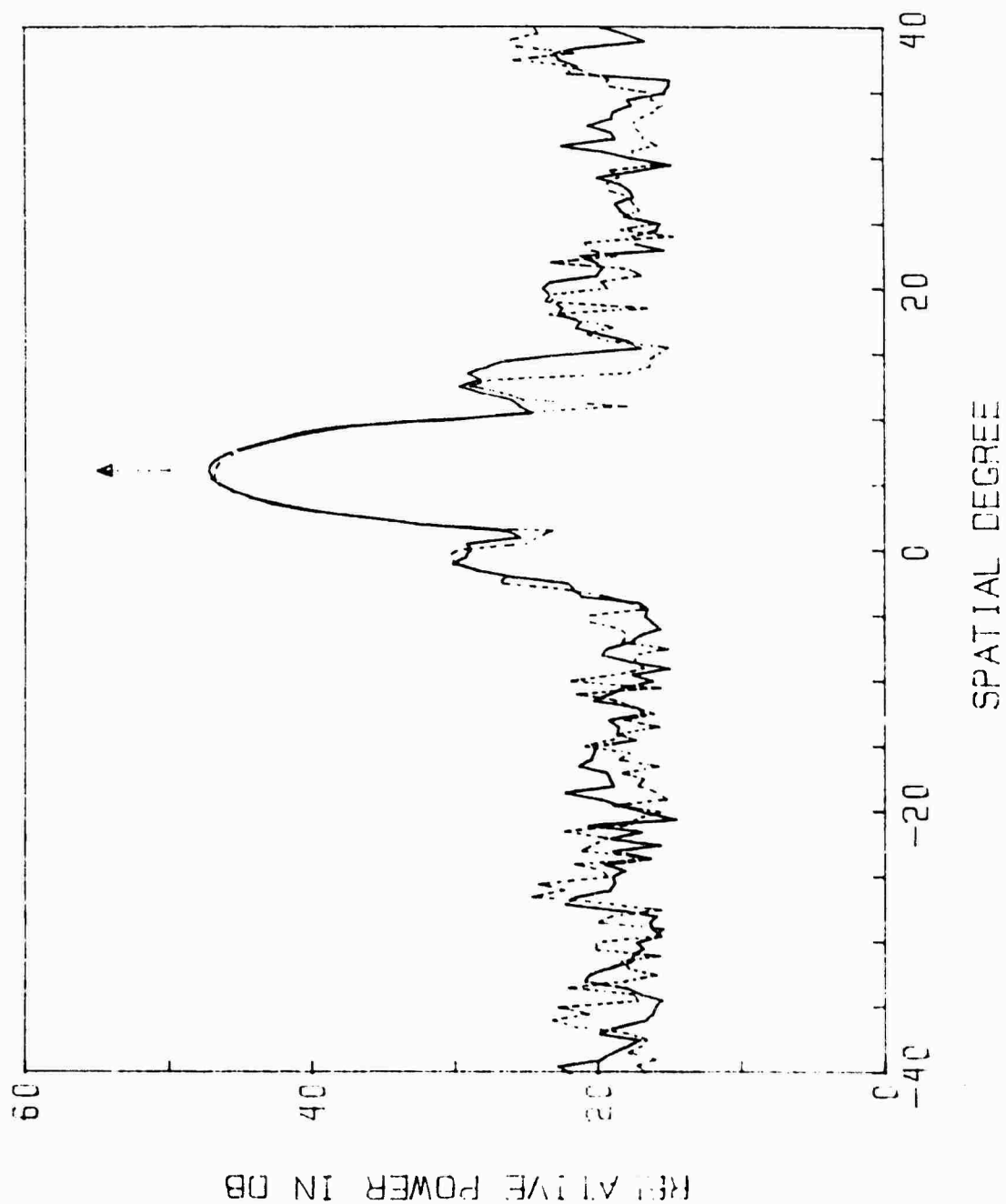elements were more than 50% of the theoretical values.

Fig. 7 Antenna patterns constructed with estimated (solid curve) and
ideal (broken curve) values of RF phase shifts and tuning phases.
The ideal values are defined as $\beta_{k\ell} = \ell \times 45°$ and $\phi_k = 0°$ for all
values of k and ℓ. The antenna is distortion-free. The CW source
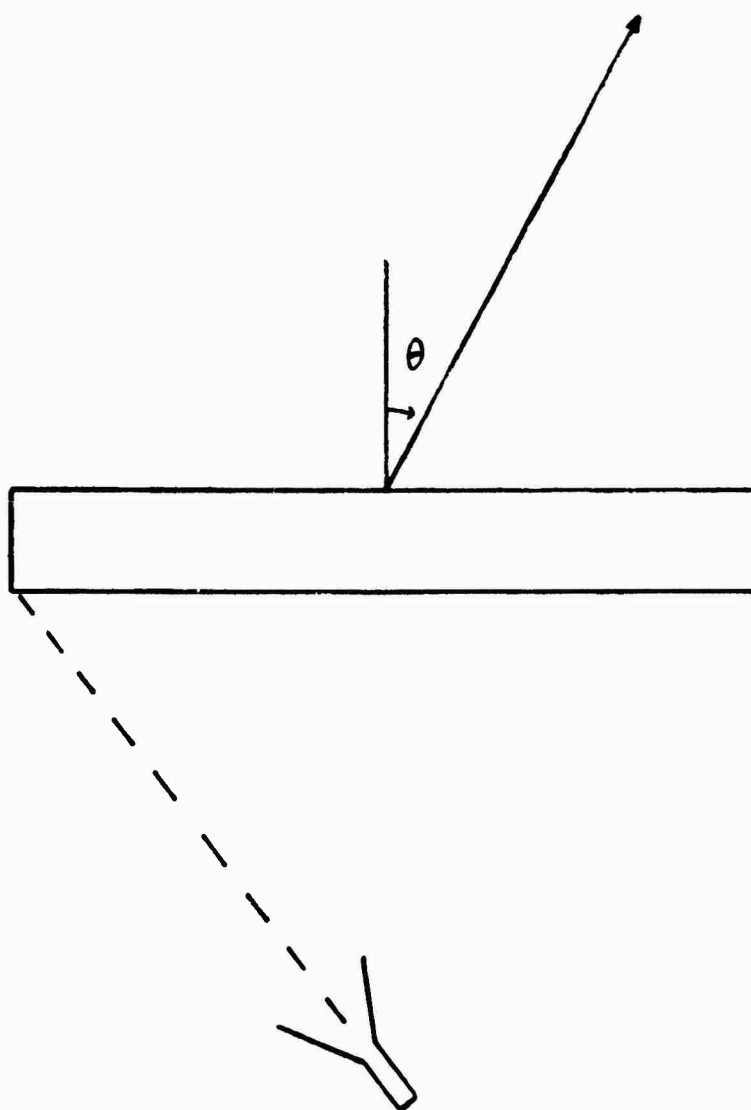direction is marked with an arrow above the antenna patterns.

Fig. 8 A diagram of the distorted antenna. The feed horn is pointed at
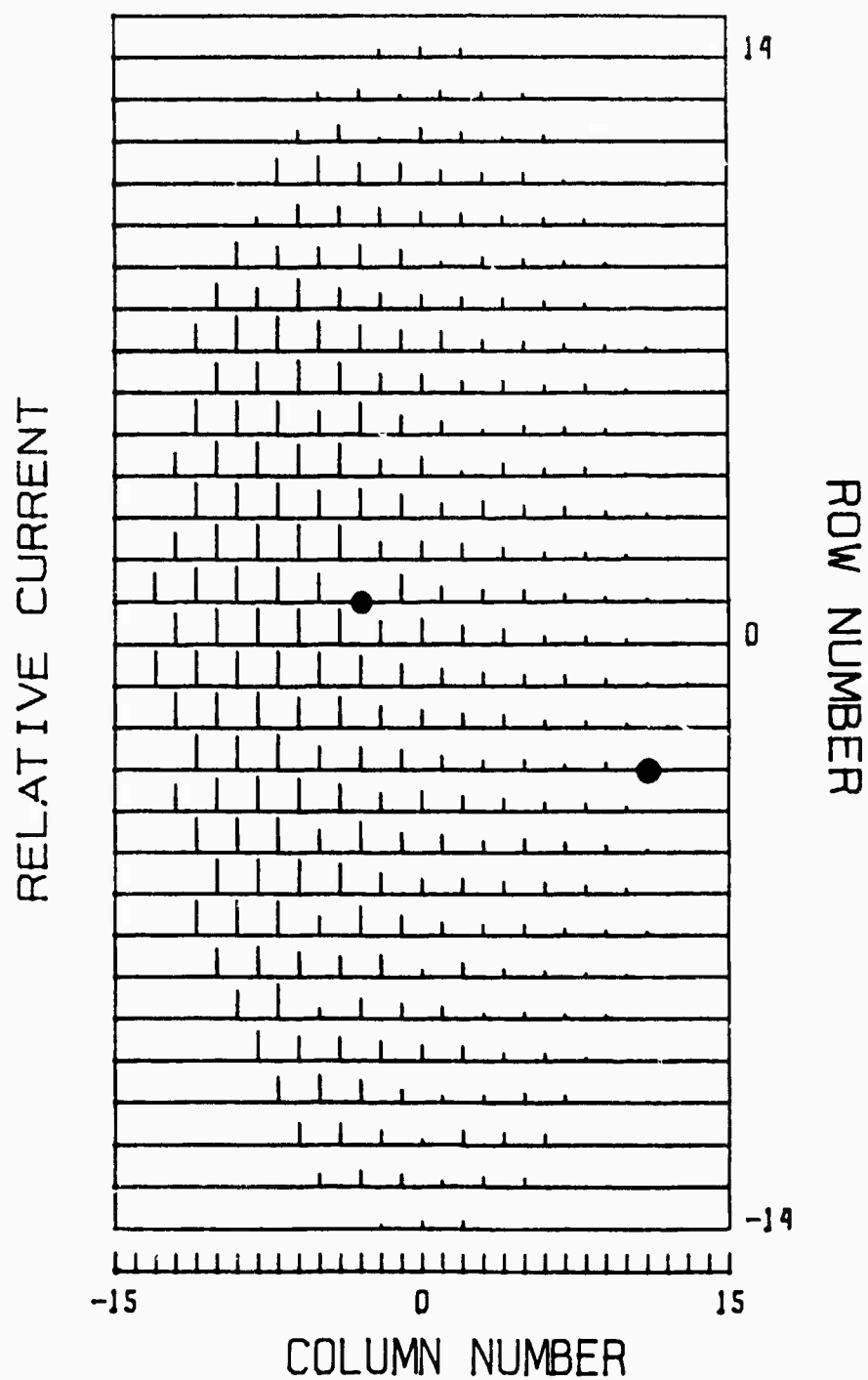   the left edge of the array.

Fig. 9   Estimates of relative array-element excitation voltages in the distorted antenna. The dots denote the positions of the defective elements.
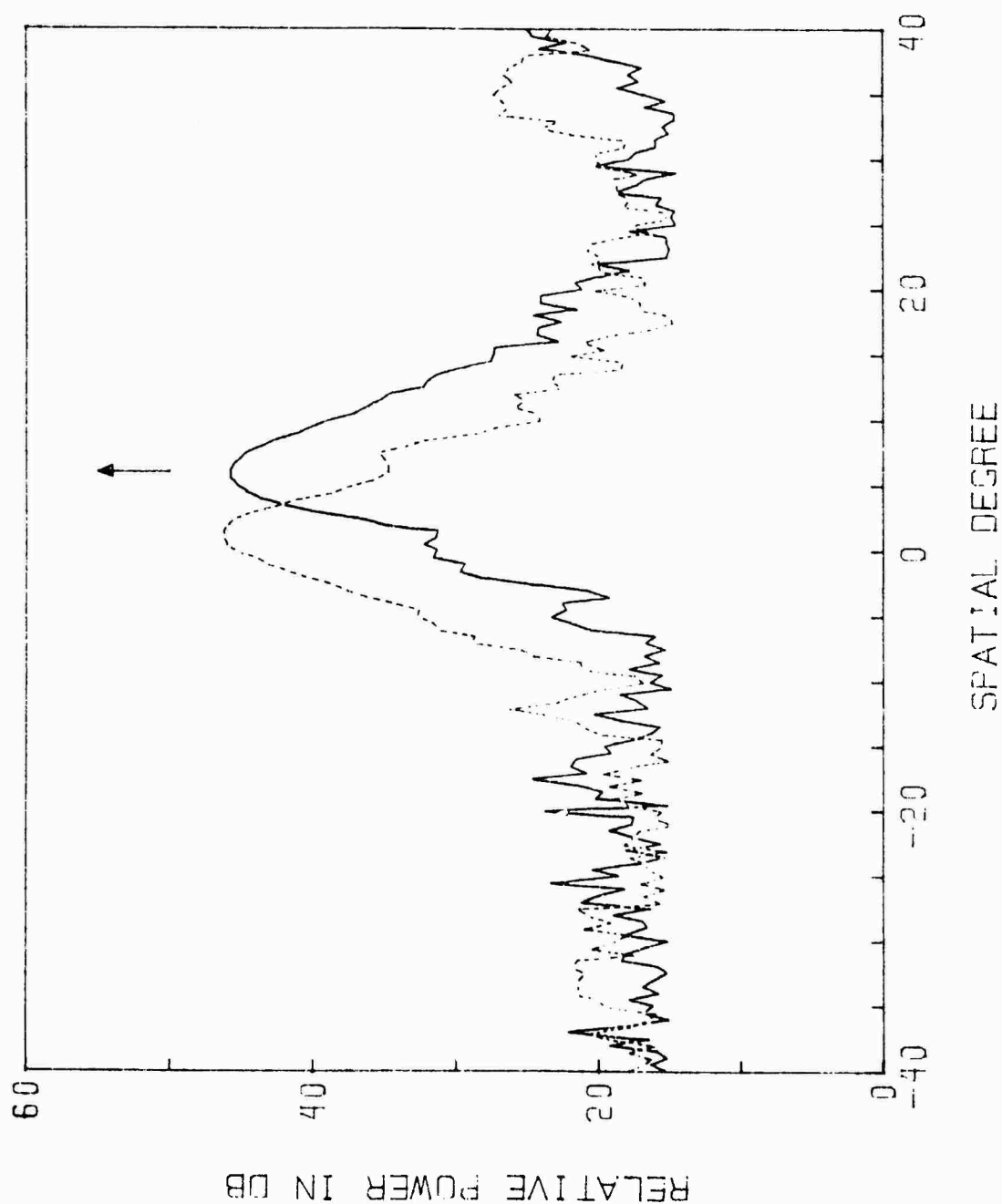
Fig. 10 Antenna patterns constructed with estimated (solid curve) and
ideal (broken curve) values of RF phase shifts and tuning phases.
The feed horn is pointed at the left edge of the array. The CW
source direction is marked with an arrow above the antenna
patterns. Note that the peak of the broken curve is in the wrong
position.

The results in Figs. 9 and 10 were consistent with the distortion of the antenna. The feed horn was pointed at the left edge of the array. Therefore, its coupling with the array elements on the left was stronger than its coupling with those on the right. This explains why the excitation voltages on the left were larger than those on the right. The rate of decrease in excitation voltage from left to right was rather rapid, and resulted in a reduction in the effective aperture of the array. This aperture reduction was the main reason for the broader beams shown in Fig. 10. A qualitative explanation for the position of the main lobe in the broken curve is now given. In Fig. 8, the opening of the feed horn was farther away from the right hand side of the array than the left. The compensation for this longer distance was essentially the same as the compensation required to steer a beam of a distortion-free antenna to the left of the boresight direction. Hence, the main lobe of the beam pattern constructed with the ideal values of $\beta_{k\ell}$ and ϕ_k was on the left of the correct position.

VII SUMMARY

A technique to measure the relative array element excitation voltages, tuning phases, and RF phase shifts of a phased-array antennas has been described. In experiments with a phased-array antenna at the Communications Research Centre in Ottawa, Canada, the estimates of relative excitation voltages were found to be in good agreement with theoretical values. The estimates of RF phase shifts were also in good agreement with bench-measured values. Antenna patterns constructed with the estimates of RF phase shifts and tuning phases also had their main lobes pointed at the CW test source.

ACKNOWLEDGEMENTS

REFERENCES

1. O. Lowenschuss, "Method and apparatus for testing phased array antennas," U.S. Patent 3,378,846, April 1968.

2. G. Hüschelrath and W. Sander, "The ELRA phased-array radar with automatic phase adjustment in practice," AGARD Conference Proc. No. 197 on New Devices, Techniques and Systems in Radar, Paper No. 36, June 1976.

3. D.K. Alexander and R.P. Gray, Jr., "Computer-aided fault determination for an advanced phased array antenna," Proceedings of 1979 Antenna Applications Symposium, University of Illinois.

4. P.J. Kahrilas and D.M. Jahn, "Hardpoint demonstration array radar," Supplement to IEEE Transactions on Aerospace and Electronic Systems, vol. AES-2, No. 6, pp. 286-299, Nov. 1966.

5. C. Blake, L. Schwartzman, and F.J. Esposito, "Evaluation of large phased-array antennas," 1970 Phased-Array Antenna Symposium, June 2-5, 1970, Polytechnic Institute of Brooklyn, Farmingdale, New York, pp. 329-331.

APPENDIX A

AN ALGORITHM TO DETERMINE THE BEST-FIT CIRCLE THROUGH
A SET OF POINTS IN THE ARGAND DIAGRAM

The best-fit circle through a set of points $\{A_{k\ell}; \ell=0,1,2,\ldots,7\}$ in the Argand diagram is identified here as the circle which minimizes the sum

$$S = \sum_{\ell=0}^{7} (d_{k\ell}^2 - a_k^2)^2 \quad .$$

where $d_{k\ell}$ is the distance of $A_{k\ell}$ from the centre $\hat{B}_k$ of the circle and a_k is the circle radius. Distance $d_{k\ell}$ is given by

$$d_{k\ell}^2 = (A_{k\ell} - \hat{B}_k)^2$$

$$= (x_\ell - x_b)^2 + (y_\ell - y_b)^2 \quad , \tag{A.2}$$

where

$$(x_\ell, y_\ell) = (\text{Re}(A_{k\ell}), \text{Im}(A_{k\ell})) \quad , \tag{A.3}$$

and

$$(x_b, y_b) = (\text{Re}(\hat{B}_k), \text{Im}(\hat{B}_k)) \quad . \tag{A.4}$$

Minimization of S in (A.1) with respect to a_k yields

$$\frac{\delta S}{\delta a_k} = 4a_k \sum_{\ell=0}^{7} [(x_\ell - x_b)^2 + (y_\ell - y_b)^2 - a_k^2] \tag{A.5}$$

$$= 0 \quad ,$$

which leads to

$$2\overline{x}x_b + 2\overline{y}y_b = (\overline{x^2} + \overline{y^2}) + (x_b^2 + y_b^2 - a_k^2) \quad , \tag{A.6}$$

where

$$\overline{x^u y^v} = \frac{1}{8} \sum_{\ell=0}^{7} x_\ell^u y_\ell^v \quad . \tag{A.7}$$

Similarly, minimization with respect to x_b and using (A.6) leads to

$$2\overline{x^2}\,x_c + 2\overline{xy}\,y_b = (\overline{x^3} + \overline{xy^2}) + (x_b^2 + y_b^2 - a_k^2)\overline{x} \quad . \tag{A.8}$$

Minimization with respect to y_b and using (A.6) leads to

$$2\overline{xy}\,x_c + 2\overline{y^2}\,y_b = (\overline{x^2y} + \overline{y^3}) + (x_b^2 + y_b^2 - a_k^2)\overline{y} \quad . \tag{A.9}$$

Upon elimination of $(x_b^2 + y_b^2 - a_k^2)$ from (A.6), (A.8), and (A.9),

$$2(\overline{x^2} - \overline{x}\,\overline{x})x_b + 2(\overline{xy} - \overline{x}\,\overline{y})y_b = \overline{x^3} - \overline{x}\,\overline{x^2} + \overline{xy^2} - \overline{x}\,\overline{y^2} \quad , \tag{A.10}$$

and

$$2(\overline{xy} - \overline{x}\,\overline{y})x_b + 2(\overline{y^2} - \overline{y}\,\overline{y})y_b = \overline{x^2y} - \overline{x^2}\,\overline{y} + \overline{y^3} - \overline{y}\,\overline{y^2} \quad . \tag{A.11}$$

Solving (A.10) and (A.11) for (x_b, y_b), and using (A.4) leads to (16) and and (17) Radius a_k, calculated with (A.6), (16) and (17), is given by (22).

In summary, the best-fit circle through a set of points in the Argand diagram is identified as a circle which minimizes the sum S given by (A.1). The circle centre is given by (16) and (17), and the circle radius is given by (22).

APPENDIX B

COMPUTATION OF REFINED ESTIMATES $\{\hat{\gamma}_{k\ell};\ \ell=0,1,2,\ldots,7\}$
FROM $\{\hat{\gamma}_{k\ell}^{(2)};\ \ell=0,1,2,\ldots,7\}$

In general, the improved estimates $\{\hat{\gamma}_{k\ell}^{(2)};\ \ell=0,1,2,\ldots7\}$ given by (26) do not satisfy (10). This appendix is concerned with the construction of refined estimates, denoted by $\{\hat{\gamma}_{k\ell};\ \ell=0,1,2,\ldots,7\}$ which satisfy both (9) and (10), i.e.,

$$\hat{\gamma}_{k\ell} - \hat{\gamma}_{k(\ell-4)} = \hat{\beta}_{k4}, \qquad \ell=4,5,6,7 \quad , \tag{B.1}$$

and

$$\hat{\gamma}_{k1} + \hat{\gamma}_{k2} = \hat{\gamma}_{k0} + \hat{\gamma}_{k3} \quad . \tag{B.2}$$

The refined estimates are linear combination of the $\hat{\gamma}_{k\ell}^{(2)}$s. If the $\hat{\gamma}_{k\ell}^{(2)}$s satisfy (10) already, one has $\hat{\gamma}_{k\ell} = \hat{\gamma}_{k\ell}$ for all values of ℓ. This property suggests as trial solutions

$$\hat{\gamma}_{k\ell} = \hat{\gamma}_{k\ell}^{(2)} + e_\ell \delta_k, \quad \ell=0,1,2,\ldots,7 \quad . \tag{B.3}$$

where

$$\delta_k = \hat{\gamma}_{k1}^{(2)} + \hat{\gamma}_{k2}^{(2)} - \hat{\gamma}_{k0}^{(2)} - \hat{\gamma}_{k3}^{(2)} + p_k \times 360° \quad . \tag{B.4}$$

and e_ℓ is a scaling factor to be determined. Here p_k is an integer which restricts δ_k to the range $[-180°, 180°)$. The choice of this range takes into account that δ_k is zero if (10) is already satisfied. From the symmetry properties of the subscripts on the right-hand side of (B.4), one gets

$$e_0 = -e_1 = -e_2 = e_3 \tag{B.5}$$

Substitution of (B.3) - (B.5) into (B.2) leads to

$$(1 - 4e_0)\delta_k = 0 \quad . \tag{B.6}$$

In general $\delta_k \neq 0$. Therefore, $(1-4e_o) = 0$, giving

$$e_0 = -e_1 = -e_2 = e_3 = 0.25 \qquad \qquad (B.7)$$

From (B.1), (B.3), and (26)

$$e_\ell \delta_k = \hat{\gamma}_{k\ell} - \hat{\gamma}_{k\ell}^{(2)}$$

$$= [\hat{\gamma}_{k(\ell-4)} + \hat{\beta}_{k4}] - [\hat{\gamma}_{k(\ell-4)}^{(2)} + \beta_{k4}]$$

$$= e_{\ell-4} \delta_k \quad , \qquad \qquad (B.8)$$

$$\ell = 4,5,6,7 \quad .$$

This relation, together with (B.7), gives

$$e_4 = -e_5 = -e_6 = e_7 = 0.25 \quad . \qquad \qquad (B.9)$$

In summary, improved estimates $\{\hat{\gamma}_{k\ell}; \ell=0,1,2,\ldots,7\}$ are calculated from $\{\hat{\gamma}_{k\ell}^{(2)}; \ell=0,1,2,\ldots,7\}$ via (B.3) using (B.4), (B.7) and (B.9). It may be noted that the magnitude of δ_k is a measure on the accuracy of the RF phase shift estimates. If $|\delta_{kn}|$ 6°, the estimates are usually very accurate. However, if $|\delta_k|$ 90°, the errors in the estimates are usually very large.

ARRAY ELEMENT		RF PHASE SHIFT $\beta_{k\ell}$ (DEGREES)					
k	(ROW, COL.)	ESTIMATED			BENCH-MEASURED		
		$\ell=1$	2	4	1	2	4
121	(2 , 0)	47	89	166	49	94	170
148	(0 , 0)	49	84	175	48	88	173
175	(-2 , 0)	48	85	167	49	90	169
141	(1 , 13)	48	104	189	49	104	194
168	(-1 , 13)	45	104	196	44	103	193

TABLE I: Independent RF phase shifts obtained by estimation and by bench measurements

DOCUMENT CONTROL DATA - R & D

(Security classification of title, body of abstract and indexing annotation must be entered when the overall document is classified)

1. ORIGINATING ACTIVITY	2a. DOCUMENT SECURITY CLASSIFICATION
Defence Research Establishment Ottawa	UNCLASSIFIED
Department of National Defence	2b. GROUP
Ottawa, Ontario, K1A 0Z4	

3. DOCUMENT TITLE

The In-Situ Calibration of a Bilateral Space-Fed Phased Array Antenna (U)

4. DESCRIPTIVE NOTES (Type of report and inclusive dates)

CRC Report

5. AUTHOR(S) (Last name, first name, middle initial)

E.K.L. Hung, N.R. Fines, R.M. Turner

6. DOCUMENT DATE	7a. TOTAL NO. OF PAGES	7b. NO. OF REFS
June 1983	33	5

8a. PROJECT OR GRANT NO.	9a. ORIGINATOR'S DOCUMENT NUMBER(S)
33C69	CRC Report No. 1370
8b. CONTRACT NO.	9b. OTHER DOCUMENT NO.(S) (Any other numbers that may be assigned this document)

10. DISTRIBUTION STATEMENT

Unlimited

11. SUPPLEMENTARY NOTES	12. SPONSORING ACTIVITY
	DREO

13. ABSTRACT

This report describes an in-situ technique to estimate the following parameters of a phased-array antenna:

1. the relative array-element excitation voltages,
2. the array-element tuning phases, and
3. the RF phase shifts at the array elements.

This technique has several significant features. First, it involves the use of two auxiliary antennas. One is a remote CW source directed at the phased-array antenna. The other is a passive antenna mounted close to the phased-array antenna. Its output is used to produce a reference phase for phase measurements. Second, it contains a technique to reduce the errors in phase estimates. Third, it takes note that beam steering uses phase sums of the form $(\phi_k + \beta_{k\ell})$, where ϕ_k is the tuning phase for the k-th array element and $\beta_{k\ell}$ is an RF phase shift of the array element, and pays special attention to reduce the errors associated with the estimates of these sums. Fourth, it assumes the use of a reasonably stable and strong CW source of commercially available quality. No other assumptions are made.

Experimental results obtained with a 295-element S-band space-fed phased-array antenna are given.

36

UNCLASSIFIED

Security Classification

KEY WORDS

In-Situ
Calibration
Antenna

INSTRUCTIONS

1 ORIGINATING ACTIVITY Enter the name and address of the organization issuing the document.

2a. DOCUMENT SECURITY CLASSIFICATION Enter the overall security classification of the document including special warning terms whenever applicable.

2b. GROUP Enter security reclassification group number. The three groups are defined in Appendix 'M' of the DRB Security Regulations.

3. DOCUMENT TITLE Enter the complete document title in all capital letters. Titles in all cases should be unclassified. If a sufficiently descriptive title cannot be selected without classification, show title classification with the usual one-capital-letter abbreviation in parentheses immediately following the title.

4 DESCRIPTIVE NOTES: Enter the category of document, e.g. technical report, technical note or technical letter. If appropriate, enter the type of document, e.g. interim, progress, summary, annual or final. Give the inclusive dates when a specific reporting period is covered

5. AUTHOR(S): Enter the name(s) of author(s) as shown on or in the document. Enter last name, first name, middle initial. If military, show rank. The name of the principal author is an absolute minimum requirement

6. DOCUMENT DATE. Enter the date (month, year) of Establishment approval for publication of the document.

7a TOTAL NUMBER OF PAGES The total page count should follow normal pagination procedures, i.e., enter the number of pages containing information

7h. NUMBER OF REFERENCES Enter the total number of references cited in the document

8a PROJECT OR GRANT NUMBER If appropriate, enter the applicable research and development project or grant number under which the document was written.

8b. CONTRACT NUMBER If appropriate, enter the applicable number under which the document was written.

9a. ORIGINATOR'S DOCUMENT NUMBER(S) Enter the official document number by which the document will be identified and controlled by the originating activity This number must be unique to this document

9b. OTHER DOCUMENT NUMBER(S). If the document has been assigned any other document numbers (either by the originator or by the sponsor), also enter this number(s).

10. DISTRIBUTION STATEMENT Enter any limitations on further dissemination of the document, other than those imposed by security classification, using standard statements such as:

(1) "Qualified requesters may obtain copies of this document from their defence documentation center."

(2) "Announcement and dissemination of this document is not authorized without prior approval from originating activity "

11. SUPPLEMENTARY NOTES Use for additional explanatory notes.

12. SPONSORING ACTIVITY. Enter the name of the departmental project office or laboratory sponsoring the research and development. Include address.

13. ABSTRACT: Enter an abstract giving a brief and factual summary of the document, even though it may also appear elsewhere in the body of the document itself. It is highly desirable that the abstract of classified documents be unclassified. Each paragraph of the abstract shall end with an indication of the security classification of the information in the paragraph (unless the document itself is unclassified) represented as (TS), (S), (C), (R), or (U).

The length of the abstract should be limited to 20 single-spaced standard typewritten lines, 7½ inches long.

14 KEY WORDS: Key words are technically meaningful terms or short phrases that characterize a document and could be helpful in cataloging the document. Key words should be selected so that no security classification is required. Identifiers, such as equipment model designation, trade name, military project code name, geographic location, may be used as key words but will be followed by an indication of technical context.